

Testing dark matter with high-redshift supernovae

Elsbeth M. Minty, Alan F. Heavens, Michael R.S. Hawkins

Institute for Astronomy, University of Edinburgh, Royal Observatory, Blackford Hill, Edinburgh EH9 3HJ, United Kingdom

7 June 2021

ABSTRACT

Dark matter in the Universe consisting of macroscopic objects such as primordial black holes may cause gravitational lensing of distant objects. The magnification associated with lensing will lead to additional scatter in the received flux from standard candles, and too small an observed scatter could rule out compact dark matter entirely. In this letter, we show how the scatter in fluxes of distant Type 1a supernovae could be used to distinguish between models with and without lensing by macroscopic dark matter. The proposed SNAP project, with ~ 2400 supernovae in the range $0.1 \lesssim z \lesssim 1.7$, should be able to identify models at 99.9% confidence, if systematic errors are controlled. Note that this test is independent of any evolution of the mean supernova luminosity with redshift. The variances of the current Supernova Cosmology Project sample do not rule out compact lenses as dark matter: formally they favour such a population, but the significance is low, and removal of a single faint supernova from the sample reverses the conclusion.

1 INTRODUCTION

In recent years one of the classic tests of the geometry of the Universe has undergone a resurgence of interest. Type 1a supernovae are thought to act as standard candles, and therefore their Hubble diagram may be used to constrain cosmological models. Dedicated discovery and follow-up programmes (Perlmutter et al. 1997, Perlmutter et al. 1998, Schmidt et al. 1998) have established the Hubble diagram to $z \simeq 1$, leading to constraints on H_0 , Ω_m and Ω_Λ , most notably the requirement of a positive cosmological constant (Riess et al. 1999). It has long been recognised that the supernova Hubble diagram would be affected by gravitational lensing, if significant quantities of dark matter resided in the form of macroscopic compact objects (hereafter MACHOs) such as black holes (Linder, Schneider & Wagoner 1988, Rauch 1991, Holz 1998, Metcalf & Silk 1999, Perlmutter et al. 1999, Seljak & Holz 1999, Weller & Albrecht 2000, Huterer & Turner 2000). Such a population has been proposed to account for the long-term variability of quasars (Hawkins 1993).

These studies have shown that lensing can have a significant effect on the estimation of cosmological parameters, and that the distribution of supernova fluxes could be used to determine whether the dark matter was in MACHO form or not. Metcalf & Silk (1999) showed that, provided the cosmology was known, microscopic dark matter could be distinguished from MACHOs with relatively small numbers of supernovae. The reason for this sensitivity is that in a MACHO-dominated universe of reasonable density, most bunches of light rays do not undergo large magnifications, and the most probable flux received is close to that expected in empty-beam models (Dyer & Roeder 1974). This shifts the most probable Hubble diagram systematically, changing the estimates of the cosmological parameters (Holz 1998). Given that one does not know the underlying cosmology, one should estimate simultaneously the background cosmology as well as the contribution to the matter density by MACHOs. This is ambitious, and will surely be attempted once larger supernova searches such as those proposed by

the Supernova/Acceleration Probe (SNAP: see <http://snap.lbl.gov>) and by the Visible and Infrared Telescope for Astronomy (VISTA; <http://www.vista.ac.uk>) are underway. In this paper, the study is more limited; we focus on how the extra scatter in supernova fluxes, from lensing, can be used to constrain the quantity of MACHO dark matter. The variance will have contributions from intrinsic variations in supernova properties, instrumental error, and lensing. The first two of these should be virtually independent of the cosmological model; the presence or absence of significant additional scatter allows a test of whether the dark matter is in the form of MACHOs.

The detectability of dark matter candidates in this test rests on how accurately the variance can be estimated from sets of supernovae. For gaussian distributions, this is readily done, but, although it may be a reasonable approximation to model the intrinsic and instrumental effects as gaussian, the lensing effect is highly skewed towards rare high-magnification events. We must therefore take care in modelling this effect accurately. We use numerical ray-tracing simulations (described in section 2) and analyse the results using a Bayesian method (section 2.1). Lensing induces an extra scatter which rises with redshift, contributing as much as 0.5 magnitudes at a redshift 1.5 for an Einstein-de Sitter model with all the matter in MACHOs. This is readily distinguishable from a no-lensing model, provided sufficient supernovae are available. We find, in general, that with ~ 2400 supernovae selected from $0.1 \lesssim z \lesssim 1.7$, as proposed by SNAP, the scatter alone can select between several cosmological models at 99.9% confidence level, if systematic errors are controlled. Note that this test has the advantage that it is insensitive to any evolution in the mean luminosity of supernova (although it is dependent on any evolution in the scatter of intrinsic properties). Similar conclusions to ours have recently been reached via a slightly different analysis by (Mortsell, Goobar & Bergstrom 2001).

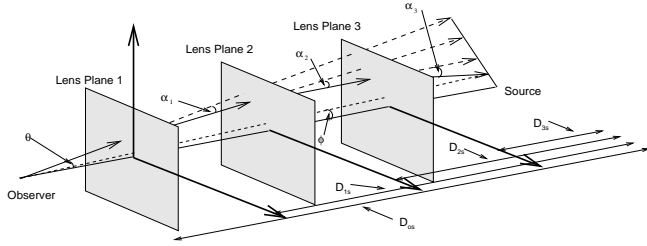


Figure 1. The ray-tracing simulation geometry. In practice we use 5 planes, but test with more.

2 METHOD

The microlensing effect on the brightness of supernovae at redshifts ~ 1 is not necessarily accurately modelled by a single-scattering event. We therefore simulate the lensing of distant supernovae with a ray-tracing program. We assume the Universe is populated with compact dark matter candidates of a single mass. The results are independent of the mass, provided the source is small compared to the Einstein radius (for canonical expansion speeds, at maximum light this is $\sim 10^{13}m$, which requires $M \gtrsim 10^{-2}M_{\odot}$). The masses are confined to a discrete set of lens planes, and rays are passed from the observer to the source plane, being bent at each stage by the lenses in each plane. The bend angle is the vector sum of the bends from individual lenses, and is computed using the Barnes-Hut tree code (Barnes & Hut 1986). The bend angle for each lens is directed towards each lens, with magnitude $\alpha = \frac{4GM}{rc^2}$ where r is the impact parameter. The rays are traced to the source redshift, and the solid angle subtended by each of the distorted pixels is computed. Since surface brightness is conserved by the lensing process, the ratio of the solid angles of the image plane pixel and distorted source plane pixel gives the magnification. Full details of the simulations will appear elsewhere (Minty et al. in preparation), but in summary we use 400–5000 lenses in total, randomly placed on 5 planes located to give equal numbers of lenses per plane. The random hypothesis is justified in Holz & Wald (1998) and Metcalf (1999). Backwards rays are sent out on a 1024×1024 grid (see Fig. 1), with rays separated by a small fraction of the Einstein radius of lenses on the nearest plane, ensuring the pattern is fully sampled. In computing the bend angle, the lens pattern is assumed to be periodic. We perform tests varying the number of sources, size of lens planes, number of planes, tree-code parameters, grid size, to ensure robustness of the results. The need for numerical simulations is illustrated in fig. 2, which shows a typical lightcurve for lensing in an Einstein-de Sitter Universe, where the dark matter is all in lenses. The optical depth to lensing is high, and the magnification is not well described by a single-scattering event. We consider four separate models, one with no lensing, one an Einstein-de Sitter model with all matter in lenses, and two flat models with matter $\Omega_m = 0.3$, and cosmological constant $\Omega_{\Lambda} = 0.7$. These two models differ in the proportion of the matter in lenses. The models are detailed in table 1. We perform two analyses here, a preliminary study of the 42 high-redshift supernovae in the Supernova Cosmology Project (Perlmutter et al. 1999), and a second study investigating whether SNAP should be capable of detecting MACHOs unambiguously. In the former case, we take the errors from the observations. For the SNAP study, we assume that there is an intrinsic variation in supernovae properties of 0.157 mag (Perlmutter et al. 1999), and a measurement error of 0.08 mag (Metcalf & Silk 1999). These errors (in magnitude) are assumed to be gaussian, and independent of redshift and cosmology, although these assumptions could be relaxed if desired. Model

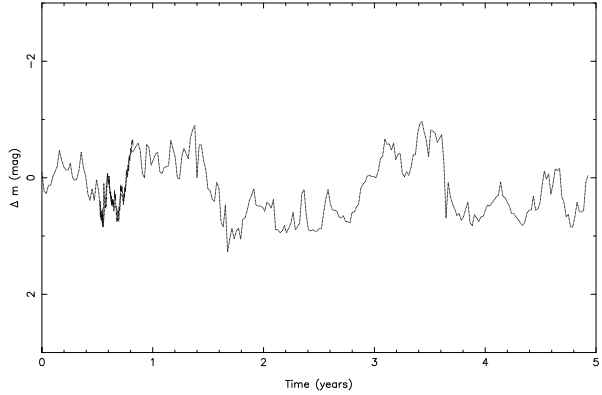


Figure 2. A sample simulated lightcurve of a supernova at $z = 1.7$ in an Einstein-de Sitter universe dominated by MACHOs. The timescale is set by the mass of lenses and their velocity dispersion; for the purposes of this figure, these are $10^{-4}M_{\odot}$ and 300 km s^{-1} .

Model	Matter density Ω_m	Cosmological constant Ω_{Λ}	Density in lenses Ω_{Lens}
1			0
2	0.3	0.7	0.1
3	0.3	0.7	0.3
4	1.0	0.0	1.0

Table 1. Models considered. Model 1 includes scatter only from measurement error and intrinsic variations.

1 contains only these components of variance. Fig. 3 shows the scatter in the magnitudes induced by lensing for models 2–4, as a function of redshift. Given that the intrinsic plus instrumental scatter is ~ 0.2 mag, we see that the additional variance from lensing becomes very significant at redshifts $\gtrsim 1$.

2.1 Statistics

SNAP proposes to obtain $N \sim 100 - 300$ supernovae per redshift interval of $\Delta z = 0.1$ between $z = 0.4$ and $z = 1.2$, with small numbers at lower and higher redshift (up to $z \sim 1.7$; see the Science Case in <http://snap.lbl.gov> for full details). For statistical analysis, we use the r.m.s. in supernova magnitude in each redshift bin. The discriminatory power is thus determined by how accurately the r.m.s. can be estimated from N supernovae. This can be calculated analytically for gaussian distributions, but the distribution of magnifications induced by lensing is far from gaussian (see fig. 4). We therefore draw N magnifications at random from the lensing simulations, noting that the probability of a supernova lying in a distorted pixel in the source plane is proportional to the solid angle of the pixel. These magnifications are applied to magnitudes drawn from gaussian distributions of variance $\sigma^2 = \sigma_{intrinsic}^2 + \sigma_{observational}^2$. For the proposed SNAP survey we take $\sigma_{intrinsic} = 0.157$ mag (Perlmutter et al. 1999) and $\sigma_{observational} = 0.08$ mag (Metcalf & Silk 1999). For the current data, we take σ to be the individual estimated r.m.s. (Perlmutter et al. 1999). We do this repeatedly, and compute the distribution of the sample variance as a function of redshift. Some representative distributions are shown in fig. 5. We compute the probability distribution of the variance estimator $D_i = \sum_j (m_{j,i} - \bar{m}_i)^2 / (N - 1)$,

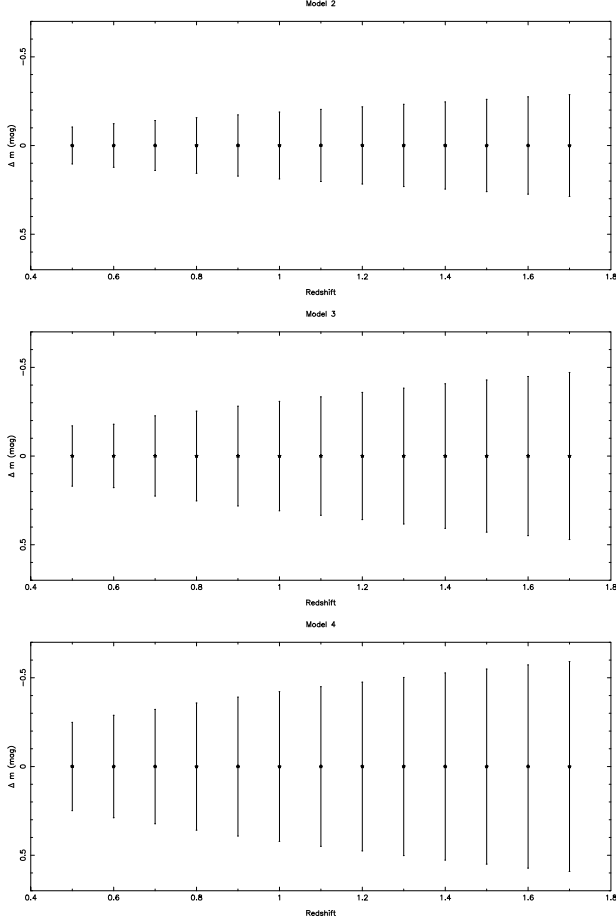


Figure 3. Mean and r.m.s. deviation of supernova brightness vs. redshift, due to lensing alone. Note that the scatter has been symmetrised. The models have, from the top, $(\Omega_0, \Omega_\Lambda, \Omega_{Lens}) = (0.3, 0.7, 0.1)$, $(0.3, 0.7, 0.3)$ and $(1.0, 0.0, 1.0)$.

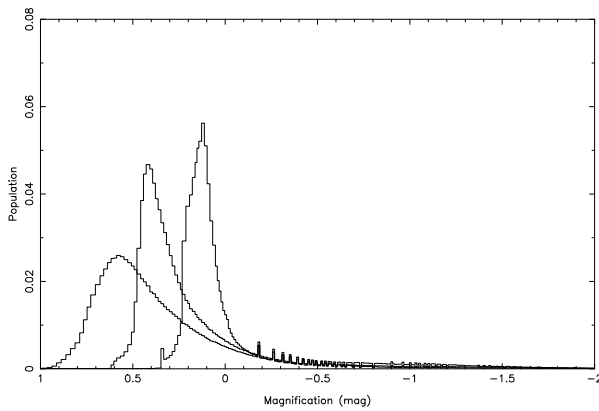


Figure 4. The distribution of magnifications arising from lensing in the three lensing models at redshift $z = 1.7$. Models 2-4, with increasing Ω_{Lens} , from the left.

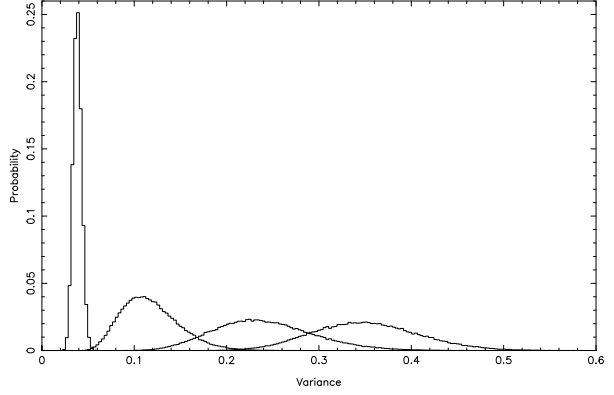


Figure 5. The distribution of the r.m.s. scatter of $N = 150$ supernovae at redshift $z = 1.7$, for the four models (1–4, from the left).

where the sum extends over $j = 1 \dots N$ supernovae in a redshift bin i . \bar{m}_i is the mean magnitude in bin i . We do this by Monte-Carlo simulation of N supernovae drawn from ray-tracing simulations. This gives us, for a given model M_k , the probability of obtaining a set of variances $\{D_i\}$,

$$p(\{D_i\}|M_k, N) = \prod_i p(D_i|M_k, N) \quad (1)$$

since the bins are independent. From now on, we suppress the N in these probabilities.

A complication arising for our analysis of future surveys is the inevitable absence of data. We seek the probability of deducing the correct model M_{cor} . Marginalising over the (unknown at this stage) true model, this is

$$\begin{aligned} p(M_{cor}) &= \sum_k p(M_{cor}, M_k) = \sum_k p(M_{cor}|M_k)p(M_k) \\ &= \frac{1}{N_k} \sum_k p(M_{cor}|M_k) \end{aligned} \quad (2)$$

where the last step follows if we assume equal prior probabilities for the true model. N_k is the number of models considered.

To compute the conditional probability in the last equation, we use the distribution of sets of variances $\{D_i\}$, given that the true model is M_t :

$$p(M_{cor}|M_t) = \int d\{D_i\} p(M_{cor}|\{D_i\}) p(\{D_i\}|M_t) \quad (4)$$

Using Bayes' theorem,

$$p(M_k|\{D_i\}) = \frac{p(\{D_i\}|M_k)p(M_k)}{p(\{D_i\})} \quad (5)$$

we see that the probability of getting the correct model, given a set of data is

$$p(M_{cor}|\{D_i\}) = \frac{p(\{D_i\}|M_t)p(M_t)}{\sum_k p(\{D_i\}|M_k)p(M_k)} \quad (6)$$

where the evidence $p(\{D_i\})$ cancels out top and bottom. If we assume uniform priors for the models, the probability simplifies, and substitution into (4) gives

$$p(M_{cor}|M_t) = \int \frac{p(\{D_i\}|M_t)^2}{\sum_k p(\{D_i\}|M_k)p(M_k)} d\{D_i\} \quad (7)$$

Redshift	Number of supernovae	Variance
0.45-0.55	11	0.064
0.55-0.65	8	0.170
0.65-0.75	3	0.076
0.75-0.85	3	0.043

Table 2. Estimated variances in supernova apparent magnitudes for four redshift bins. Data from the Supernova Cosmology Project (Perlmutter et al. 1999).

Model	Ω_m	Ω_Λ	Ω_{Lens}	Relative likelihood	SN1997K removed
1			0	0.58	1.0
2	0.3	0.7	0.1	0.92	0.88
3	0.3	0.7	0.3	0.96	0.66
4	1.0	0.0	1.0	1.0	0.32

Table 3. Relative likelihood for the four models, from the high-redshift supernovae observed as part of the supernova cosmology project.

In practice we approximate the integral over sets of data by a set of N_r random drawings (labelled by α):

$$p(M_{cor}) = \frac{1}{N_k} \sum_{M_t} \frac{1}{N_r} \sum_{\alpha} \left[\frac{p(\{D_i\}_{\alpha}|M_t)}{\sum_k p(\{D_i\}_{\alpha}|M_k)p(M_k)} \right]. \quad (8)$$

We compute this probability for varying numbers of supernovae per unit redshift interval.

3 RESULTS

For the existing 42 high-redshift supernovae published from the Supernova Cosmology Project (Perlmutter et al. 1999), we can compute the relative likelihood of the four models considered. For the data, we use the stretch luminosity-corrected effective B-band magnitude. We subtract from it the expected magnitude for model 2 (or 3), and compute the variance (using the standard estimator) for 4 bins between $z = 0.45$ and $z = 0.85$. The reason for the subtraction is that the redshift bins for which we have microlensing amplification distributions are quite broad, and the mean apparent magnitude is expected to vary substantially over the bin. For the Einstein-de Sitter model, the additional variance from subtracting the wrong evolution is negligible. The variances in the four bins are shown in table 2. Various effects conspire to make the $0.55 < z < 0.65$ bin the crucial one: first, at lower redshift, the lensing makes little difference to the variance; second, at higher redshift, there are very few supernovae in the bins; finally, the observed variance is high in the second bin. Thus the second redshift bin favours models with more microlensing, since the expected no-lensing variance is only 0.04. Combining the results gives the relative likelihoods shown in table 3, where the likelihood of the favoured model is set to unity. We see that the variances in the data have a slight preference for a population of MACHOs, but the significance is low. In fact removing a single supernova (SN1997K) from the dataset reduces the variance to 0.053, reversing the conclusions and making the no-lensing model the preferred choice (see table 3). There is little *a priori* justification for removing this point. In fact it is anomalously faint, so it is not a good candidate lensing event. Thus, unsurprisingly, we are unable to learn much from this test on current data.

		Number of supernovae per $\Delta z = 0.1$					
	25	50	75	100	125	150	175
True Model: 1 ($\Omega_{Lens} = 0$)							
1	0.998	1.000	1.000	1.000	1.000	1.000	1.000
2	0.002	0.000	0.000	0.000	0.000	0.000	0.000
3	0.000	0.000	0.000	0.000	0.000	0.000	0.000
4	0.000	0.000	0.000	0.000	0.000	0.000	0.000
True Model: 2 ($\Omega_m = 0.3, \Omega_\Lambda = 0.7, \Omega_{Lens} = 0.1$)							
1	0.004	0.000	0.000	0.000	0.000	0.000	0.000
2	0.927	0.986	0.996	0.998	0.999	1.000	1.000
3	0.069	0.014	0.004	0.002	0.001	0.000	0.000
4	0.000	0.000	0.000	0.000	0.000	0.000	0.000
True Model: 3 ($\Omega_m = 0.3, \Omega_\Lambda = 0.7, \Omega_{Lens} = 0.3$)							
1	0.000	0.000	0.000	0.000	0.000	0.000	0.000
2	0.065	0.014	0.004	0.002	0.001	0.000	0.000
3	0.838	0.949	0.977	0.990	0.996	0.999	1.000
4	0.097	0.037	0.019	0.008	0.002	0.001	0.000
True Model: 4 ($\Omega_m = 1.0, \Omega_\Lambda = 0, \Omega_{Lens} = 1.0$)							
1	0.000	0.000	0.000	0.000	0.000	0.000	0.000
2	0.000	0.000	0.000	0.000	0.000	0.000	0.000
3	0.088	0.032	0.016	0.006	0.003	0.001	0.000
4	0.902	0.968	0.984	0.994	0.997	0.999	1.000

Table 4. Probability of deducing, from the four considered, correct and incorrect models given the true model. Probabilities $< 5 \times 10^{-4}$ are set to zero for this table. The redshift distribution is assumed to be uniform across $0.1 < z < 1.7$.

Future experiments should be able to do this task well. In table 4, we show the conditional probabilities of selecting models, given a correct model, for experiments with a flat redshift distribution of supernovae in the range $0.1 - 1.7$. Probabilities less than 0.0005 are set to zero in the table. In fig. 6 we show how the probability of obtaining the correct model changes as we increase the number of sources per $\Delta z = 0.1$ bin. We assume here a uniform prior: i.e. all models are equally likely *a priori*. SNAP's expected redshift distribution is not uniform, but rises towards $z = 1.2$ with a small number of supernovae extending to $z = 1.7$. Using the expected redshift distribution from a one-year SNAP experiment (see Science Case in <http://snap.lbl.gov>), the conditional probabilities of selecting correct and incorrect models are given in table 5. Basically SNAP should be able to do this test very well; there is only a very small possibility of confusing the $\Omega_{Lens} = 0.3$ model with higher and lower lens densities. Combined with a uniform prior for the models, the probability of selecting the correct model is 99.9%. In this paper, we have only considered a discrete number of lensing models. A full Fisher matrix analysis of the error expected on the MACHO contribution is possible if many lensing simulations are run, or a good fitting formula is used for the magnification probability, but it is clear from this study that SNAP should be able to constrain the dark matter nature extremely well.

4 CONCLUSIONS

We have demonstrated how the scatter in the supernova fluxes can be used to support or rule out models with MACHO dark matter. Lensing by MACHOs increases the variance in the fluxes, and for models with a high density in MACHO dark matter, the variance can be increased by a factor greater than 3 at redshifts accessible

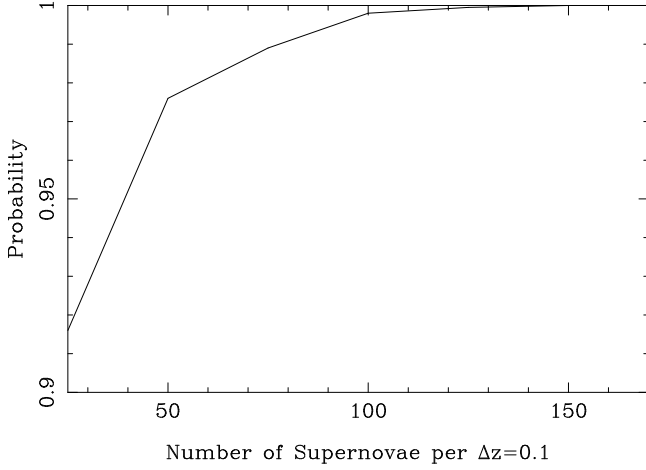


Figure 6. The probability of obtaining the correct model, plotted against the number of supernovae per redshift interval $\Delta z = 0.1$. In all cases it is assumed that supernovae are observed up to $z = 1.7$.

True Model	Trial Model	$p(\text{Trial Model} \text{True Model})$
1	1	1.0
	2	2×10^{-11}
	3	0.0
	4	0.0
2	1	0.0
	2	0.9999
	3	6×10^{-5}
	4	0.0
3	1	0.0
	2	0.002
	3	0.994
	4	0.003
4	1	0.0
	2	0.0
	3	0.0004
	4	0.9996

Table 5. Probabilities of proposed 1-year SNAP mission distinguishing between lensing and no-lensing models. Model parameters are given in table 1.

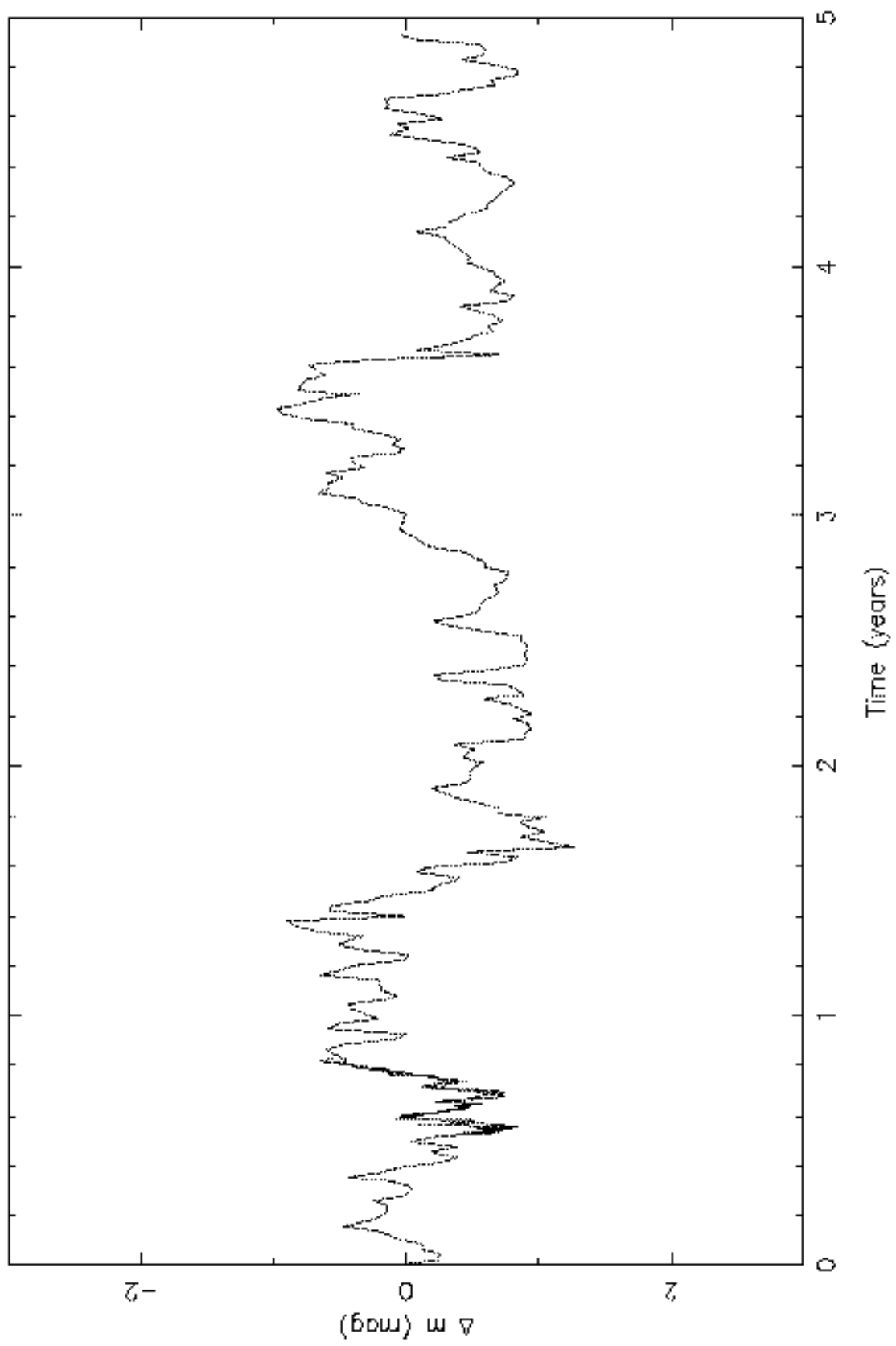
by supernova searches. Simply put, if the observed variance in supernova magnitudes is too small, it can eliminate MACHOs as the dominant dark matter candidate. The existing data from the Supernova Cosmology Project data do not rule out MACHOs, and conclusions about whether MACHOs are preferred or not are sensitive to inclusion or exclusion of individual supernovae. Future planned surveys, such as the proposed SNAP survey should be able to distinguish models readily, and in principle provide an accurate measurement of the quantity of MACHO dark matter.

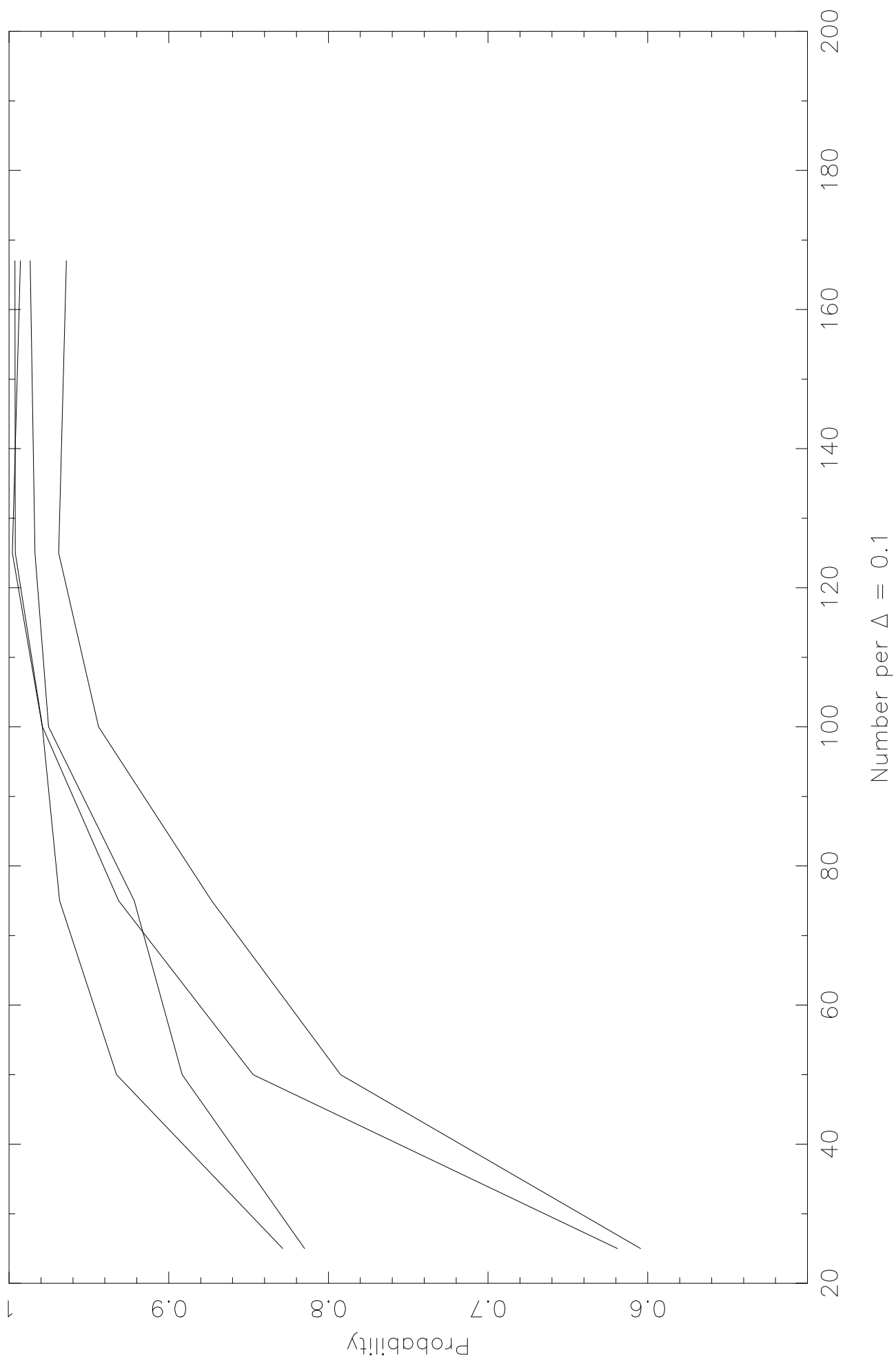
Acknowledgments

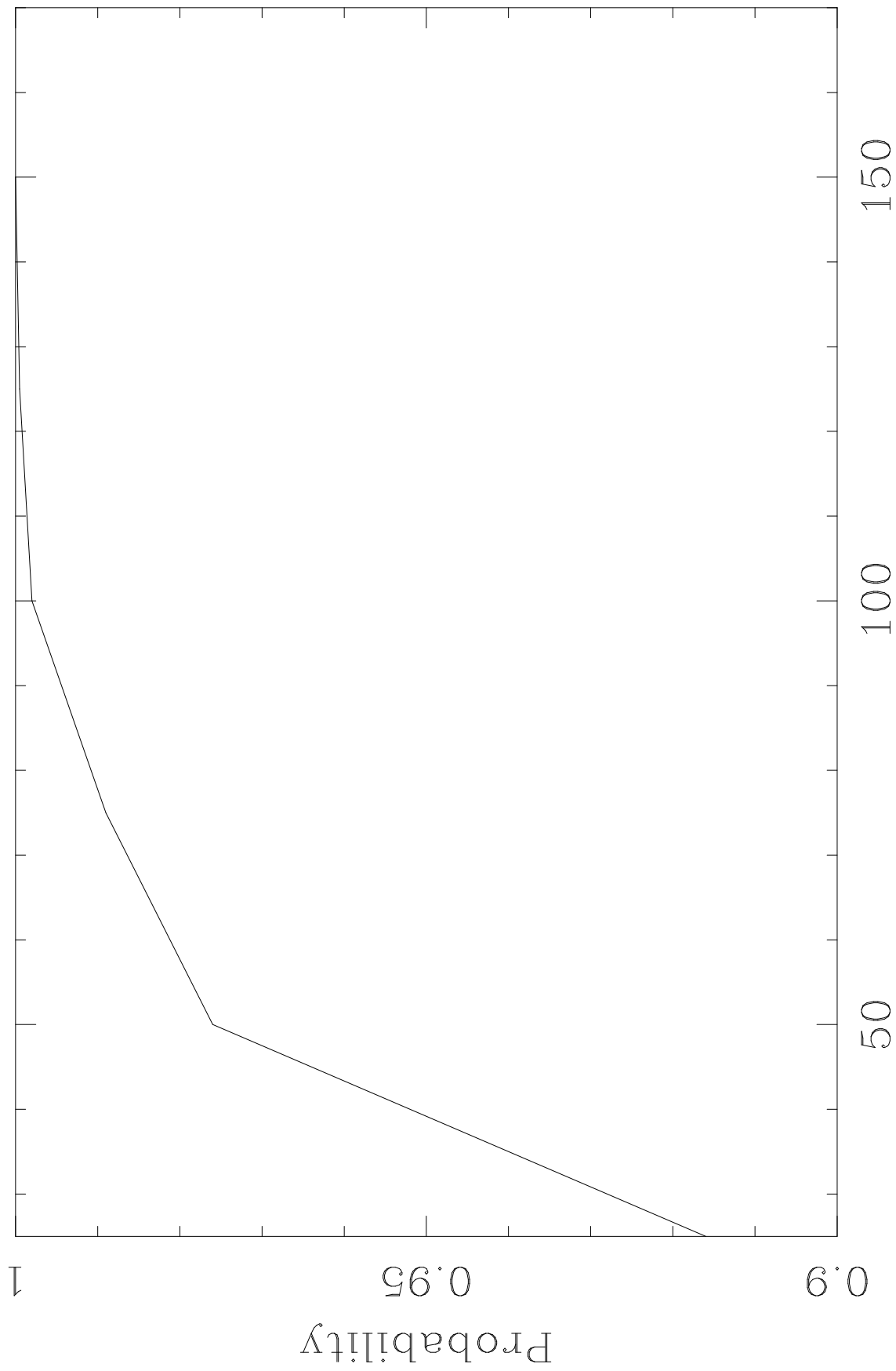
We are grateful to Isobel Hook and Andy Taylor for useful discussions, and to the High Performance Computer Group, Hitachi Europe Ltd, on whose machines some of the simulations were run.

REFERENCES

- Barnes J., Hut P., 1986. *Nat.*, 324, 446.
Dyer C. C., Roeder R. C., 1974. *ApJ*, 189, 167.
Hawkins M. R. S., 1993. *Nat.*, 366, 242.
Holz D., Wald R., 1998. *Phys. Rev. D*, 58, 063501.
Holz D., 1998. *ApJ(Lett)*, 506, L1.
Huterer D., Turner M. S., 2000. *astro-ph*, 0012510.
Linder E., Schneider P., Wagoner R., 1988. *ApJ*, 324, 786.
Metcalf R. B., Silk J., 1999. *ApJ(Lett)*, 519, L1.
Metcalf R. B., 1999. *MNRAS*, 305, 746.
Mortsell E., Goobar A., Bergstrom L., 2001. *astro-ph*, 0103489.
Perlmutter et al. S., 1997. *ApJ*, 483, 565.
Perlmutter et al. S., 1998. *Nat.*, 391, 51.
Perlmutter et al. S., 1999. *ApJ*, 517, 565.
Rauch K. P., 1991. *ApJ*, 374, 83.
Riess et al. A. G., 1999. *AJ*, 116, 1009.
Schmidt et al. B. P., 1998. *ApJ*, 507, 46.
Seljak U., Holz D., 1999. *A&A*, 351, L10.
Weller J., Albrecht A., 2000. *astro-ph*, 0008314.







Number of Supernovae per $\Delta z=0.1$